ENVIRONMENTAL RESEARCH
LETTERS

LETTER • OPEN ACCESS

Future climate change significantly alters interannual wheat yield variability over half of harvested areas

To cite this article: Weihang Liu *et al* 2021 *Environ. Res. Lett.* **16** 094045

View the article online for updates and enhancements.

ENVIRONMENTAL RESEARCH
LETTERS

LETTER

Future climate change significantly alters interannual wheat yield variability over half of harvested areas

Weihang Liu[1,2,3], Tao Ye[1,2,3,4,*] [iD], Jonas Jägermeyr[5,6,7] [iD], Christoph Müller[7] [iD], Shuo Chen[1,2,3], Xiaoyan Liu[1,2,3] and Peijun Shi[1,2,3,8]

1 Institute of Disaster Risk Science, Faculty of Geographical Science, Beijing Normal University, Beijing 100875, People's Republic of China
2 Key Laboratory of Environmental Change and Natural Disaster, Ministry of Education, Faculty of Geographical Science, Beijing Normal University, Beijing 100875, People's Republic of China
3 State Key Laboratory of Earth Surface Processes and Resource Ecology, Faculty of Geographical Science, Beijing Normal University, Beijing 100875, People's Republic of China
4 The Frederick S. Pardee Center for the Study of the Longer-Range Future and Department of Earth and Environment, Boston University, Boston, MA 02215, United States of America
5 NASA Goddard Institute for Space Studies, New York, NY 10025, United States of America
6 Center for Climate Systems Research, Columbia University, New York, NY 10025, United States of America
7 Potsdam Institute for Climate Impact Research (PIK), Member of the Leibniz Association, 14412 Potsdam, Germany
8 Academy of Plateau Science and Sustainability, People's Government of Qinghai Province and Beijing Normal University, Xining 810016, People's Republic of China
* Author to whom any correspondence should be addressed.

E-mail: yetao@bnu.edu.cn

Abstract

Climate change affects the spatial and temporal distribution of crop yields, which can critically impair food security across scales. A number of previous studies have assessed the impact of climate change on mean crop yield and future food availability, but much less is known about potential future changes in interannual yield variability. Here, we evaluate future changes in relative interannual global wheat yield variability (the coefficient of variation (CV)) at 0.25° spatial resolution for two representative concentration pathways (RCP4.5 and RCP8.5). A multi-model ensemble of crop model emulators based on global process-based models is used to evaluate responses to changes in temperature, precipitation, and CO_2. The results indicate that over 60% of harvested areas could experience significant changes in interannual yield variability under a high-emission scenario by the end of the 21st century (2066–2095). About 31% and 44% of harvested areas are projected to undergo significant reductions of relative yield variability under RCP4.5 and RCP8.5, respectively. In turn, wheat yield is projected to become more unstable across 23% (RCP4.5) and 18% (RCP8.5) of global harvested areas—mostly in hot or low fertilizer input regions, including some of the major breadbasket countries. The major driver of increasing yield CV change is the increase in yield standard deviation, whereas declining yield CV is mostly caused by stronger increases in mean yield than in the standard deviation. Changes in temperature are the dominant cause of change in wheat yield CVs, having a greater influence than changes in precipitation in 53% and 72% of global harvested areas by the end of the century under RCP4.5 and RCP8.5, respectively. This research highlights the potential challenges posed by increased yield variability and the need for tailored regional adaptation strategies.

1. Introduction

Interannual crop yield variability is one of the primary drivers of food system instability (IPCC 2019). Assessing the effects of climate change on yield variability is critical to understanding the impact of climate change on food security (FAO 2019). Due to trends in global warming (Lobell *et al* 2011) and the

changing frequency and intensity of climate extremes (Trnka *et al* 2014), potential decreases in the mean yields of crops and an increase in the interannual yield variability could adversely affect the livelihoods of producers, create spikes in food prices, lead to hunger (IPCC 2014), and even cause political instabilities at a regional level (Sternberg 2011). Previously, the impact of climate change on mean crop yield (Lobell *et al* 2011, Rosenzweig *et al* 2014) has been investigated with a focus on food availability (Campbell *et al* 2016). From a climate risk perspective, the concept of time of climate impact emergence has recently been introduced, linking mean yield changes with historical yield variability (Jägermeyr *et al* 2021). Yet, the impact of climate change on future interannual yield variability has not received sufficient attention (Wheeler *et al* 2013, Challinor *et al* 2014).

Interannual yield variability has always been one of the key risk indicators of crop production. Early studies have either assumed a stationary process without considering variability changes (Ray *et al* 2015, Ceglar *et al* 2016, Tao *et al* 2016, Matiu *et al* 2017) or linked changes in variability to non-climatic factors (Kucharik and Ramankutty 2005, Döring and Reckling 2018, Knapp and Van Der Heijden 2018, Müller *et al* 2018). Recent studies have provided evidence for changes in the interannual yield variability of major cereal crops and identified significant impacts of climate change at the global scale 0.5° grid level or at the country level (Osborne and Wheeler 2013, Iizumi and Ramankutty 2016). These studies have been followed up by regional, county-level analyses of the interannual yield variability of maize (Hawkins *et al* 2013, Lobell *et al* 2014, Leng 2017). Efforts have also been devoted to projecting the impact of future climate change on interannual yield variability, focusing on wheat and maize at global and regional scales, using process-based crop models (Moriondo *et al* 2011, Liu *et al* 2019) and statistical models (Urban *et al* 2012, Ben-Ari *et al* 2018, Tigchelaar *et al* 2018). Results from these studies have indicated substantial changes in interannual yield variability as a result of climate change, and that the sign and magnitude of change varies by production region.

Climate-related risk assessment on crop yield requires reflecting the spatial heterogeneity of both agricultural systems and climate change effects relevant for interannual yield variability (Benami *et al* 2021). There are still major research gaps in our understanding of these linkages across regions. In terms of major staple crops, only changes in yield coefficient of variation (CV) of wheat (Liu *et al* 2019) and maize have been analysed (Tigchelaar *et al* 2018) at the global scale. As these studies have used either site-based simulation or globally homogeneous warming perturbations, it is difficult to deduce robust conclusions on changes in interannual yield variability, reflecting the spatial heterogeneity of climate projections (Leng and Hall 2020). In addition,

although the mechanism of impact and the mean yield response to change in climate drivers (e.g. temperature, precipitation, and CO_2) have been intensively discussed (Schlenker and Roberts 2009, Zhu *et al* 2019), the response of interannual yield variability to changes in the various climate drivers is not well understood.

The aim of this study is to evaluate potential changes in interannual wheat yield variability under two climate change scenarios globally, and to attribute individual contributions of temperature, precipitation, and CO_2. The main research questions are: (a) How could climate change affect interannual wheat yield variability on current wheat-growing areas by the end of the century? (b) How much of these changes can be attributed to changes in temperature, precipitation, and their interaction, respectively? (c) To what extent can elevated CO_2 concentrations mitigate potential increases in yield variability? Answers to these questions will provide crucial information for climate risk assessment and effective adaptation measures.

We address these questions by conducting multi-model ensemble simulations with crop model emulators forced with global climate projections at high spatial resolution (0.25°). Statistical crop model emulators are developed based on simulations from global gridded crop models (GGCMs), facilitated by AgMIP's Global Gridded Crop Model Intercomparison Project (GGCMI). Crop model emulators have recently gained popularity as a powerful tool for assessing the impact of climate change on crop yield (Lobell and Burke 2010, Holzkämper *et al* 2012, Oyebamiji *et al* 2015, Raimondo *et al* 2021, Müller *et al* 2021). Emulators substantially improve computational efficiency and reduce data-processing requirements compared to running the original models, without sacrificing much prediction performance (Blanc and Sultan 2015, Blanc 2017, Folberth *et al* 2019, Franke *et al* 2020a, Ringeval *et al* 2021). The use of a large ensemble of GCM projections in combination with the ensemble of crop yield emulators allows for comprehensively evaluating changes in future yield variability and the associated distribution of extreme yield levels.

2. Materials and methods

2.1. Input data
2.1.1. Gridded crop model data for emulator construction
The input and output data for the simulation of global gridded wheat yield were obtained from the GGCMI phase 2 experiment dataset (Franke *et al* 2020b). The spatial resolution of this dataset is 0.5°. The input data included four different data types, i.e. climate, soil, atmospheric CO_2 concentration, and nitrogen fertilizer application rates (table S1 (available online at stacks.iop.org/ERL/16/094045/mmedia),

Franke *et al* 2020b). Baseline climate inputs were used from the AgMIP Modern-Era Retrospective Analysis for Research and Applications (AgMERRA) forcing dataset (1980–2010), including daily maximum and minimum temperatures, precipitation, and solar radiation (Ruane *et al* 2015). Based on these baseline reference simulations, the GGCMI phase 2 experiment used systematic perturbations in each grid cell with seven temperature levels (from −1 K to +6 K in 1 K interval, with +5 K skipped), nine precipitation levels (from −50% to +30%, in 10% interval, with −40% skipped), four CO_2-concentration levels (360, 510, 660, and 810 ppm), and three nitrogen levels (10, 60, and 200 kg ha^{-1}) (table S2; Franke *et al* 2020b). Twelve GGCMs were then forced with each of these perturbations of the original reanalysis weather data. The GGCMs used a national and subnational crop calendar for wheat that is based on Sacks *et al* (2010), Portmann *et al* (2010), and environment-based extrapolations (Elliott *et al* 2015).

The output data contained irrigated and rainfed yield simulations from 1980 to 2010 for each of the different perturbation levels. In this study, we selected 8 out of the 12 crop models in the GGCMI phase 2 experiment for constructing the emulators. These were APSIM-UGOE, EPIC-IIASA, EPIC-TAMU, GEPIC, LPJ-GUESS, LPJmL, pDSSAT, and PEPIC. CARAIB was not included as it did not consider nitrogen stress. ORCHIDEE-crop was not included as it did not provide simulation results for spring wheat. PROMET and JULES were not included as they used different climate inputs. Although these eight crop models differed in their representation of crop phenology, leaf-area development, yield formation, root expansion, and nutrient assimilation, all accounted for the effects of water and heat stress and assumed no technological change (Blanc 2017). All input and output data sets were provided by GGCMI at the standardized spatial resolution of 0.5°. More detailed descriptions of the individual crop models and the input and output data characteristics are available in the supplementary material (SM).

2.1.2. Data for emulator-based yield projections
To project a high spatial resolution global wheat yield, the Earth Exchange Global Daily Downscaled Projections (NEX-GDDP) dataset (Thrasher 2012), with a spatial resolution of 0.25°, was obtained from the National Aeronautics Space Administration (NASA). This database contains the global daily maximum/minimum near-surface air temperature and precipitation data from 21 General Circulation Models (GCMs) from the Coupled Model Intercomparison Project phase 5 (CMIP5, Taylor *et al* 2012) under two representative concentration pathways (RCP4.5 and RCP8.5), covering the years 1950–2100. Other RCPs are not available through NEX-GDDP.

The emulator-based projections used a national and subnational crop calendar for wheat from

MIRCA2000 (Portmann *et al* 2010). Given that MIRCA2000 has only monthly resolution, it was assumed that the first day of the month was the date of planting, and the last day of the month was the date of harvesting (Elliott *et al* 2015). The calendar we used to project yield was only MIRCA2000 because if we used the calendar of the GGCMI phase 2, we would be troubled with the mismatch between the separated spring and winter wheat calendar and only wheat harvested areas in spatial production allocation model (SPAM). Global wheat harvested area distribution around the year 2005 was obtained from the SPAM for rainfed and irrigated systems at five arc-minute resolution (You *et al* 2014).

2.2. Methods
The methodologies for evaluating changes in wheat yield variability under future climate scenarios includes the following steps (figure 1): (a) Develop annual yield emulators for the process-based GGCMI crop models. (b) Conduct emulator-based yield projections based on the NEX-GDDP climate model ensemble. (c) Summarize the future changes in wheat yield variability relative to the baseline; decompose the changes in yield variability into changes in mean yield and yield standard deviation. And (d) Separate the contributions from the changes in climatic drivers to the changes in the yield variability.

2.2.1. Development of annual GGCM emulators by extreme gradient boosting (XGB)
A previous study developed emulators of climatological-mean yield based on GGCMI phase 2 experiment data (Franke *et al* 2020b). We, however, develop an emulator capable of capturing year-to-year variability in yield. A machine-learning (ML) approach was used in this study for its flexibility for data-driven development of models with high accuracy (Folberth *et al* 2019) and its associated computational efficiency.

Development of the emulator consists of training—via a ML algorithm—on specific GGCM input and output datasets, so that the emulator replicates the complex process of yield simulation within the crop model. Variables that have been frequently reported to significantly influence wheat yield were prepared as the predicting variables, including climate, soil type, length of growing season, and management practices (table S3). All the data for training were computed/adapted from the GGCMs' input and output datasets.

All prediction variables were computed/obtained from the GGCMI phase 2 data archive. The climate data are supplied as daily values and were, in a first step, aggregated to monthly sums or averages (MON). For each grid, the month of planting was defined as month 1 to harmonize, on a global basis, the order of
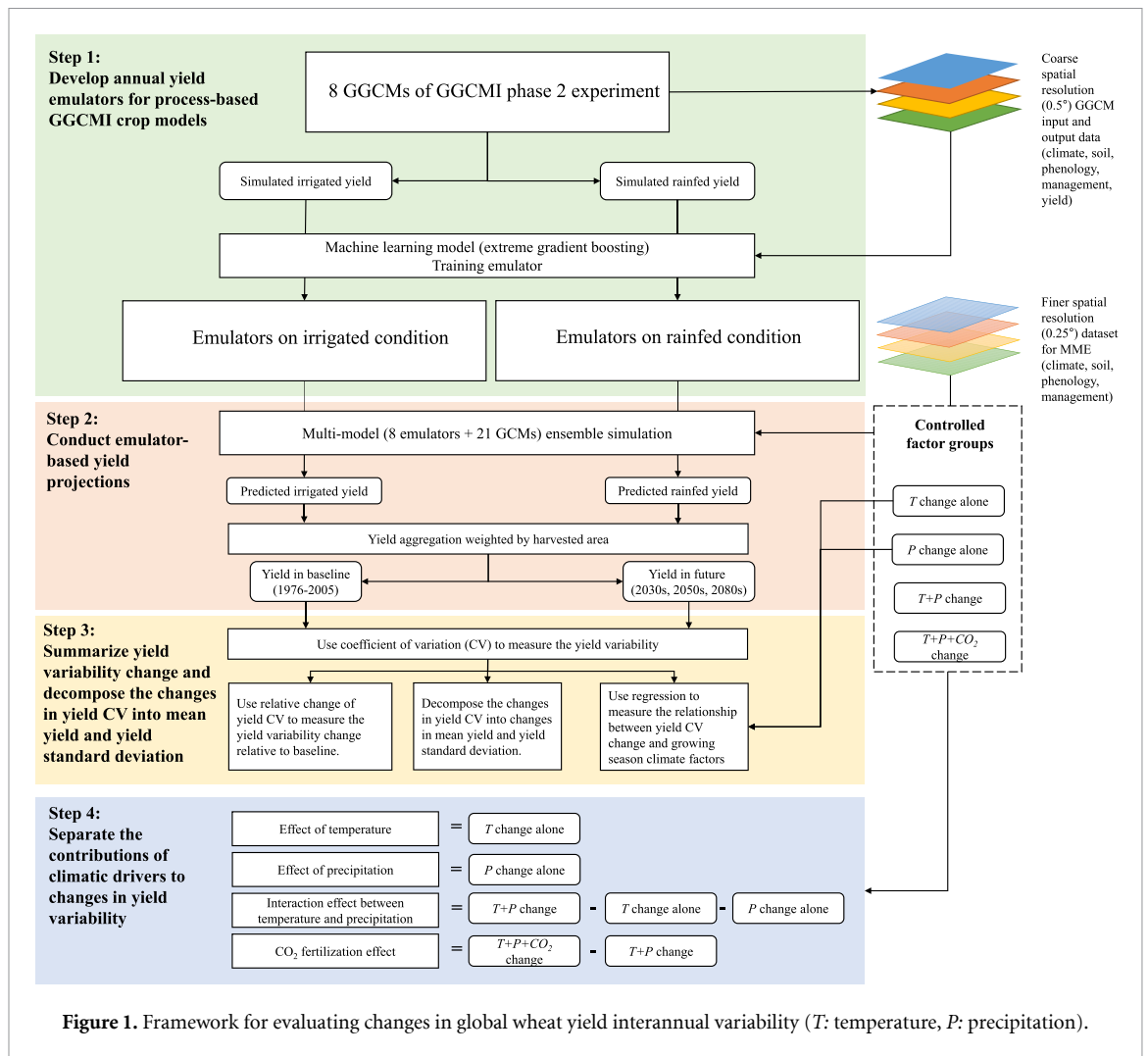
Figure 1. Framework for evaluating changes in global wheat yield interannual variability (*T:* temperature, *P:* precipitation).

months from planting. Subsequently, prediction variables were calculated for each month in the growing-season months and the entire growing season (GS, based on the planting and harvesting dates for the GGCMs). Soil properties were adopted primarily for the topsoil class. Additional characteristics like length of growing season were regarded as a cultivar characteristic. The total amount and fraction of the nitrogen fertilizer application and CO_2 concentration were uniform for each grid.

In total, 32 different emulators were trained for the eight GGCMs, each with two water management modalities (rainfed and irrigation) and two wheat types (spring wheat and winter wheat). An XGB algorithm was used due to its better performance in terms of goodness-of-fit, cross-validation errors, and computation efficiency compared with a random forest algorithm (Folberth *et al* 2019). The predicting variables and the simulated yield in the GGCMs were randomly split into training and validation sets, which contained 75% and 25% of the samples (Yue *et al* 2019), respectively. Depending on the size of the dataset supplied by each GGCM, 1.7×10^6–2.3×10^7 (0.9×10^7–1.9×10^8) samples were used for

model training and 0.6×10^6–0.8×10^7 (0.3×10^7–0.6×10^8) samples were used for validation of irrigation (rainfed) conditions, covering the period of 1981–2010. More details on emulator training, validation, and performance evaluation are available in SM and figures S1 and S2.

2.2.2. Emulator-based wheat yield projections
The emulators were then used to project global wheat yield by using future GCM projections. It is important to ensure that emulator-based projections do not exceed the range of training samples to avoid unrealistic extrapolation effects (Folberth *et al* 2019, Franke *et al* 2020b). The GGCMI phase 2 perturbations were designed to accommodate high-end warming scenarios (RCP8.5-2080s). For growing season average maximum temperature, the range of training data (interannual and spatial variability in AgMERRA + GGCMI perturbation) covered the entire range of the GCM projections. CO_2 concentrations were averaged with a 30 year moving window and the highest CO_2 concentration under RCP8.5-2080s is 760 ppm.

Table 1. Climate driver sensitivity simulations.

Climate drivers	Descriptions
'T'	Using future scenarios of temperature, other drivers taken from baseline
'P'	Using future scenarios of precipitation, other drivers taken from baseline
'T + P'	Using future scenarios of temperature and precipitation, holding CO_2 constant at 360 ppm
'T + P + CO$_2$'	Using future scenarios of temperature, precipitation, and CO_2

Ensemble yield projections were conducted at the global level for grids with a spatial resolution of 0.25° for the years 1976–2005 (baseline), 2006–2035 (2030s), 2036–2065 (2050s), and 2066–2095 (2080s) under RCPs of 4.5 and 8.5. If the spring and winter wheat are grown in parallel at national or subnational level, we determined the wheat type with larger harvested areas according to MIRCA2000 (Portmann *et al* 2010). The multi-model ensemble approach improves the robustness of future climate-change impact estimates and allows for analyses of spatial heterogeneity and inter-model uncertainty (Martre *et al* 2015). There were 336 future wheat yield estimates (21 GCMs × 8 emulators × 2 RCPs), each simulated for 4 × 30 year periods. Throughout all simulations, planting dates, cultivar selection, soil properties, and management practices were assumed to remain constant over time, which is consistent with the GGCMI Phase 2 experimental design A0 (Franke *et al* 2020b), which is used for training the emulators here. Final estimates of future yield responses are based on the median across the crop model emulators and GCMs.

2.2.3. Measuring the change in yield variability
Rainfed and irrigated yield were first aggregated to grid and national levels using an area-weighted average (Müller *et al* 2017), as described in the following equation:

$$y_t = \frac{\sum\limits_{i=1}^{n} y_{i,\mathrm{firr},t} \cdot area_{\mathrm{firr}} + \sum\limits_{i=1}^{n} y_{i,\mathrm{noirr},t} \cdot area_{\mathrm{noirr}}}{\sum\limits_{i=1}^{n} (area_{\mathrm{firr}} + area_{\mathrm{noirr}})}. \quad (1)$$

where i is the index of any grid cell assigned to the spatial unit in year t, n is the number of grid cells in that spatial unit, $y_{i,\mathrm{firr},t}$ is the emulator-projected yield under fully irrigated conditions in grid cell i, and $y_{i,\mathrm{noirr},t}$ is the emulator-projected yield for rainfed conditions in grid cell i; area is the harvested area in grid cell i, either due to fully irrigated or rainfed, obtained from SPAM.

We used the CV a measure of interannual yield variability, where $CV = \sigma/\mu$, in which σ and μ are the standard deviation and mean, respectively, over a reference period. We compare the baseline period (1976–2005) with six future scenario-periods: RCP4.5-2030s, RCP4.5-2050s, RCP4.5-2080s, RCP8.5-2030s, RCP8.5-2050s, and RCP8.5-2080s. The percentage change in yield CV in one of

the six future scenario-periods relative to the baseline period is then measured by:

$$\delta_{\mathrm{scenario}} = \frac{CV_{\mathrm{scenario}} - CV_{\mathrm{baseline}}}{CV_{\mathrm{baseline}}} \times 100\%. \quad (2)$$

2.2.4. The effects of changes in temperature, precipitation, and CO_2
The effects of changes in temperature, precipitation, and CO_2 were separated by using individual climate driver perturbed simulations, with one climate factor at a time taken from a climate scenario and the rest from the baseline. Four such climate driver sensitivity simulations (table 1) were conducted to isolate the effects of changes in temperature, precipitation, their interaction effects, and the CO_2 fertilization effect.
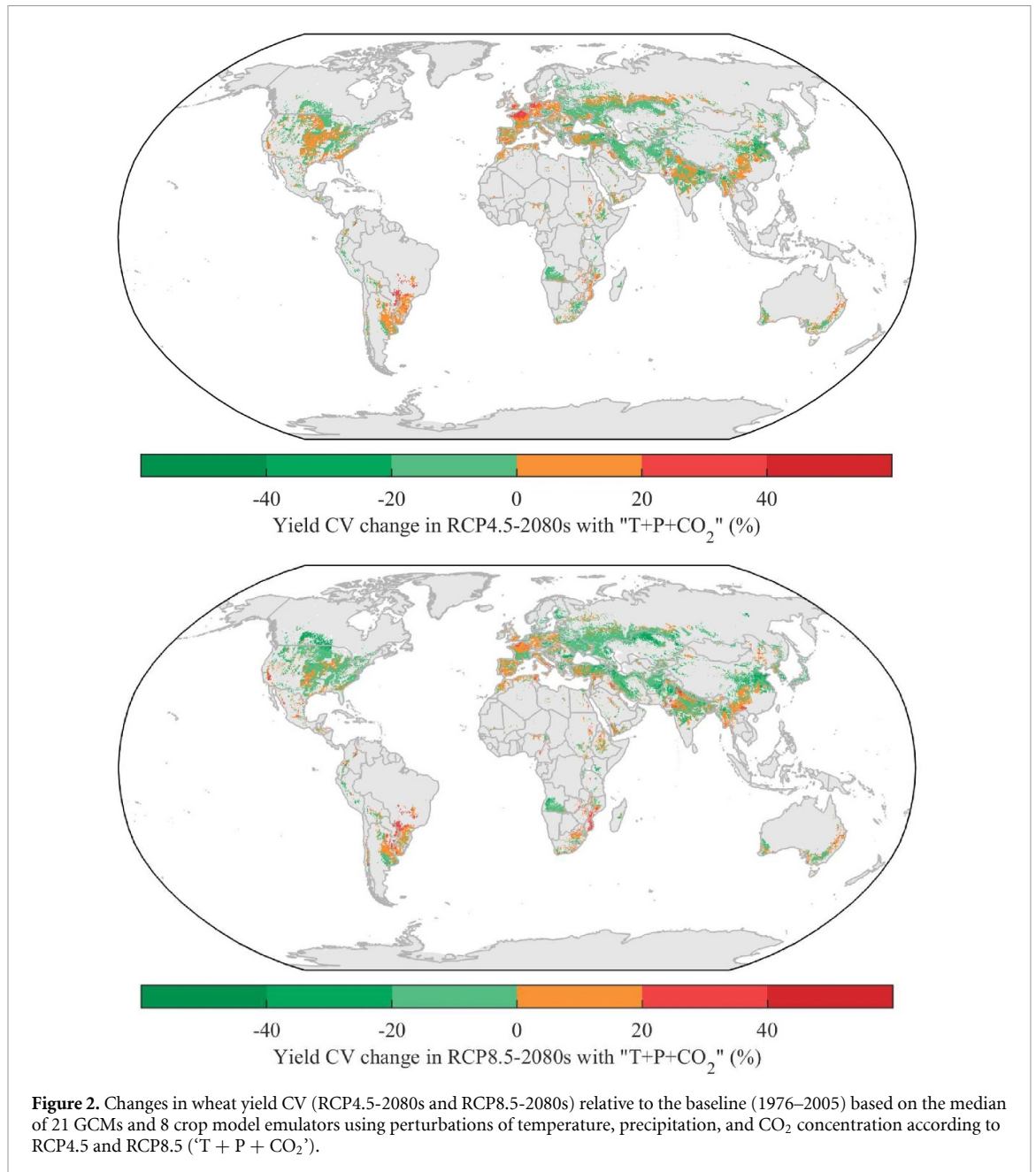
The climate driver sensitivity simulations listed in table 1 allow for addressing the following:

(a) The effects of temperature and precipitation changes can be derived by comparing the results of groups 'T' and 'P' with the baseline simulations, respectively.
(b) The interaction between temperature and precipitation changes can be evaluated using the difference between groups 'T + P' and 'T' + 'P'.
(c) The effect of CO_2 fertilization can be evaluated using the difference between groups, 'T + P + CO$_2$' and 'T + P'.

3. Results

3.1. Global patterns of future change in wheat yield interannual variability

By the end of the century, model simulations indicate an overall decrease in wheat yield CV, but in some regions, including major producing countries, there would be more unstable wheat yield (figure 2). The spatial patterns of CV changes intensify towards the end of the century, indicating a more polarized pattern under the long-term scenarios RCP4.5-2080s and RCP8.5-2080s (figure S3). Under RCP8.5-2080s, with the CO_2 fertilization effect ('T + P + CO$_2$'), the yield CV increases significantly in 18% of harvested areas ($p < 0.05$; see figure S4 for significance test), while 44% of harvested areas experience significant decrease of the yield CV ($p < 0.05$). Under RCP4.5-2080s, with the CO_2 fertilization effect ('T + P + CO$_2$'), 23% of harvested areas undergoes significant increase of yield CV ($p < 0.05$), while yield

Figure 2. Changes in wheat yield CV (RCP4.5-2080s and RCP8.5-2080s) relative to the baseline (1976–2005) based on the median of 21 GCMs and 8 crop model emulators using perturbations of temperature, precipitation, and CO_2 concentration according to RCP4.5 and RCP8.5 ('T + P + CO_2').

becomes more stable in 31% of harvested areas significantly ($p < 0.05$). Western Europe, northern Australia, central US, South Asia, Southwest China, and Myanmar are found to experience a small increase in yield CV (<40%). In eastern Europe, southern Australia, and central India yield CV is indicated to decrease by >20% under RCP8.5-2080s (figure 2). The spatial patterns of changes are consistent across different scenarios and time periods, but the size of changes varies (figure S5). The uncertainty across crop yield projections (standard deviation of CVs across all 8 emulators and 21 GCMs) ranged between 17% and 119% with the CO_2 fertilization effect, with a global mean of 39% under RCP8.5-2080s. Uncertainty was most pronounced in central Europe to eastern Russia, and in the northern Indian production

regions (figure S6). We further break the total uncertainty to those associated with the emulators and those with the GCMs, by analysis of variance. Disagreement across the emulators explained less than 50% of the total variance in 47% of the harvested areas (figure S7).

Changes in yield CV are linked to changes in mean yield and yield standard deviation. Under RCP8.5-2080s, mean yield levels increase in 92.1% of harvested areas and the yield standard deviation increases in 95.3% of harvested areas (figure S8). About 30.8% of the areas in which CV is found to increase, CV changes are dominated by increases in yield standard deviation ($|SD+| > |MY+|$). In regions where CV is decreasing, 59.3% of the areas are dominated by mean yield increases ($|SD+| < |MY+|$) (figure 3, table 2).

Figure 3. Factors of yield CV changes, including mean yield changes (MY) and yield standard deviation changes (SD). Positive changes are indicated with '+' and negative changes with '−'. The |MY+| and |SD+| denote the absolute increase of mean yield and yield standard deviation, respectively.
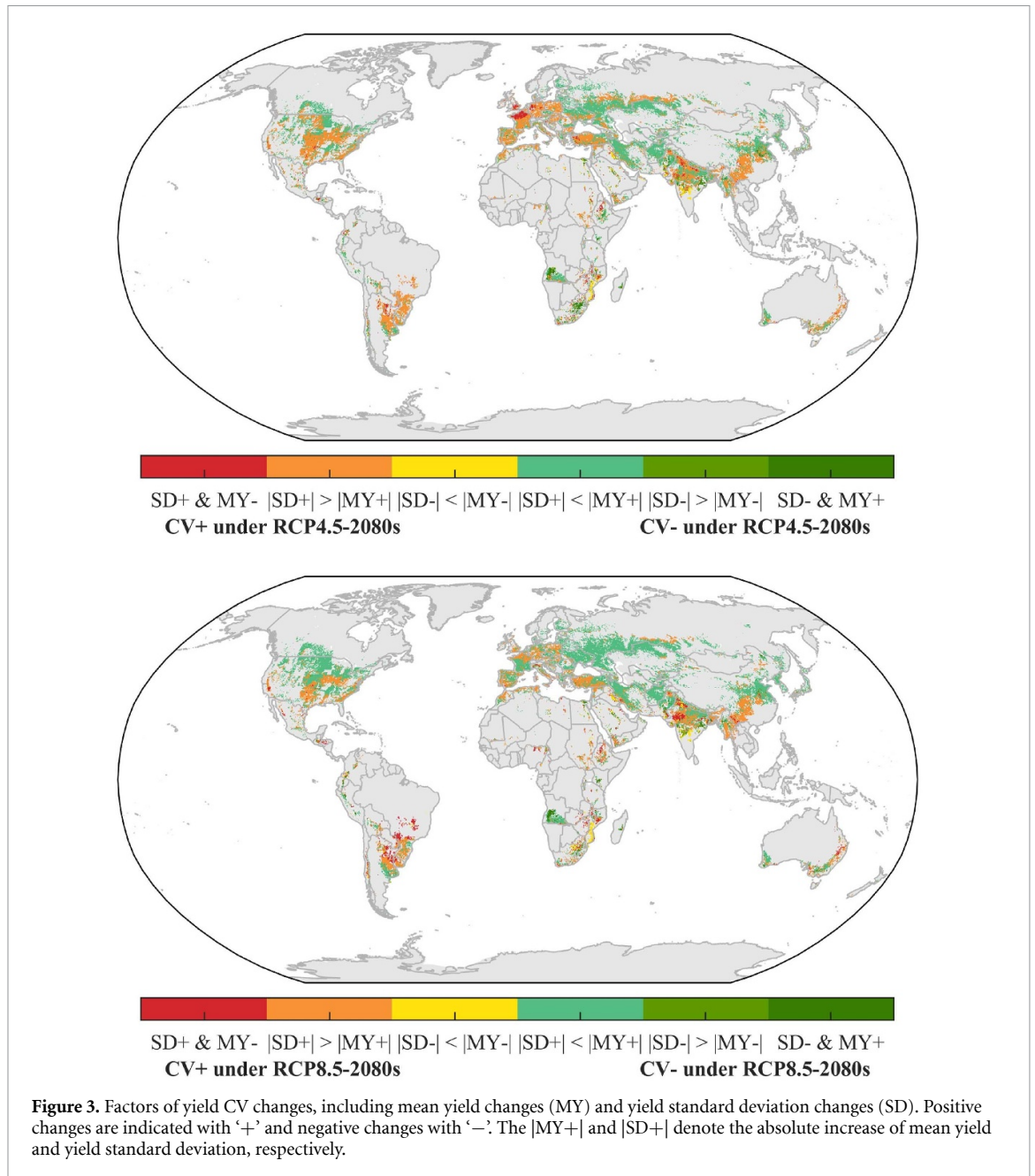
Under RCP4.5-2080s, mean yield levels and the yield standard deviation increase in 92.8% and 94.5% of the harvested areas, respectively (figure S8). About 42.7% of the areas in which CV is found to increase, CV changes are dominated by increases in yield standard deviation ($|SD+| > |MY+|$). In regions where CV is decreasing, 47.6% of the areas are dominated by mean yield increases ($|SD+| < |MY+|$) (figure 3, table 2).

3.2. Changes in the yield CV across different climatic regions

Changes in the wheat yield CV exhibited a clear relationship with the baseline regional temperature, precipitation, and nitrogen fertilizer application rate. In general, regions with hotter growing seasons (growing season average temperature > 20 °C) or with

lower nitrogen fertilizer application rates (nitrogen application rate < 200 kg ha^{-1}), experienced the largest relative increase in wheat yield CV (figure 4).

The increases in yield CV tend to be greater in regions with hotter growing seasons under both RCP4.5 and RCP8.5, including sub-Saharan Africa, India, Australia's wheat belt, South East US, and southern Brazil and Argentina. These are regions in which mean wheat yields are expected to decrease under high-emission climate change scenarios, whereas at higher latitudes with lower growing season temperatures mean wheat yields are generally projected to increase (Jägermeyr *et al* 2021). The change in yield CV undergoes smaller decline under RCP8.5 and even experiences subtle increase under RCP4.5 in regions with wetter growing seasons, which can be attributed to stronger variability of precipitation in

Table 2. Attribution of wheat harvested area with yield CV changes to changes in mean yield (MY) and standard deviation (SD) under RCP4.5-2080s and RCP8.5-2080s.

Changes in yield CV	Category of SD and MY change	Fraction of harvested areas	
		RCP4.5	RCP8.5
CV+	SD+ & MY−[a]	4.3%	5.2%
	|SD+| > |MY+|	42.7%	30.8%
	|SD−| < |MY−|	2%	0.6%
CV−	|SD+| < |MY+|	47.6%	59.3%
	|SD−| > |MY−|	0.9%	2.1%
	SD− & MY+	2.6%	2.0%

[a] '+' denotes positive changes, and the '−' denotes negative changes. '\|SD+\| > \|MY+\|' denotes the absolute value of increase in yield SD is greater than that in the mean yield.
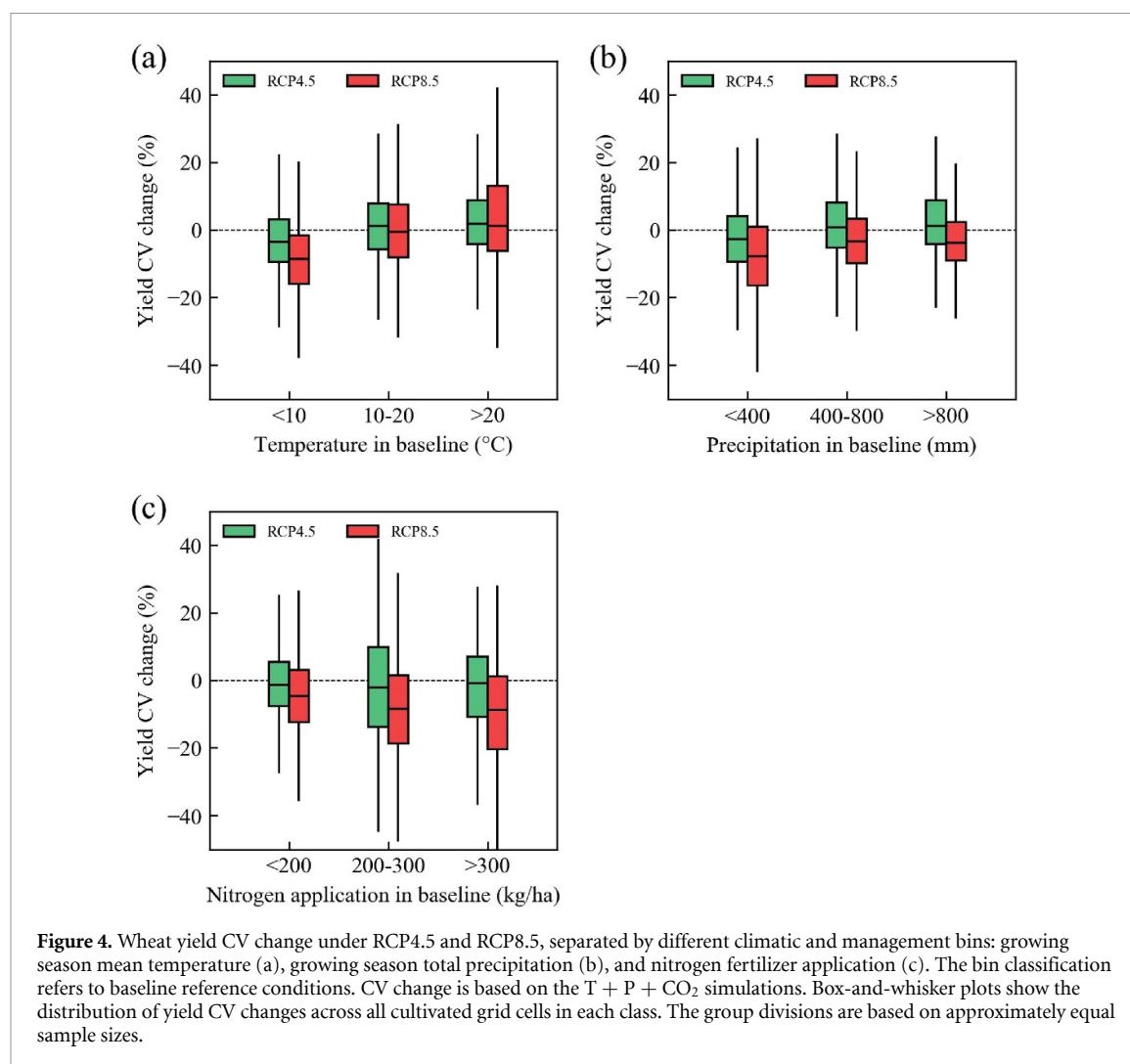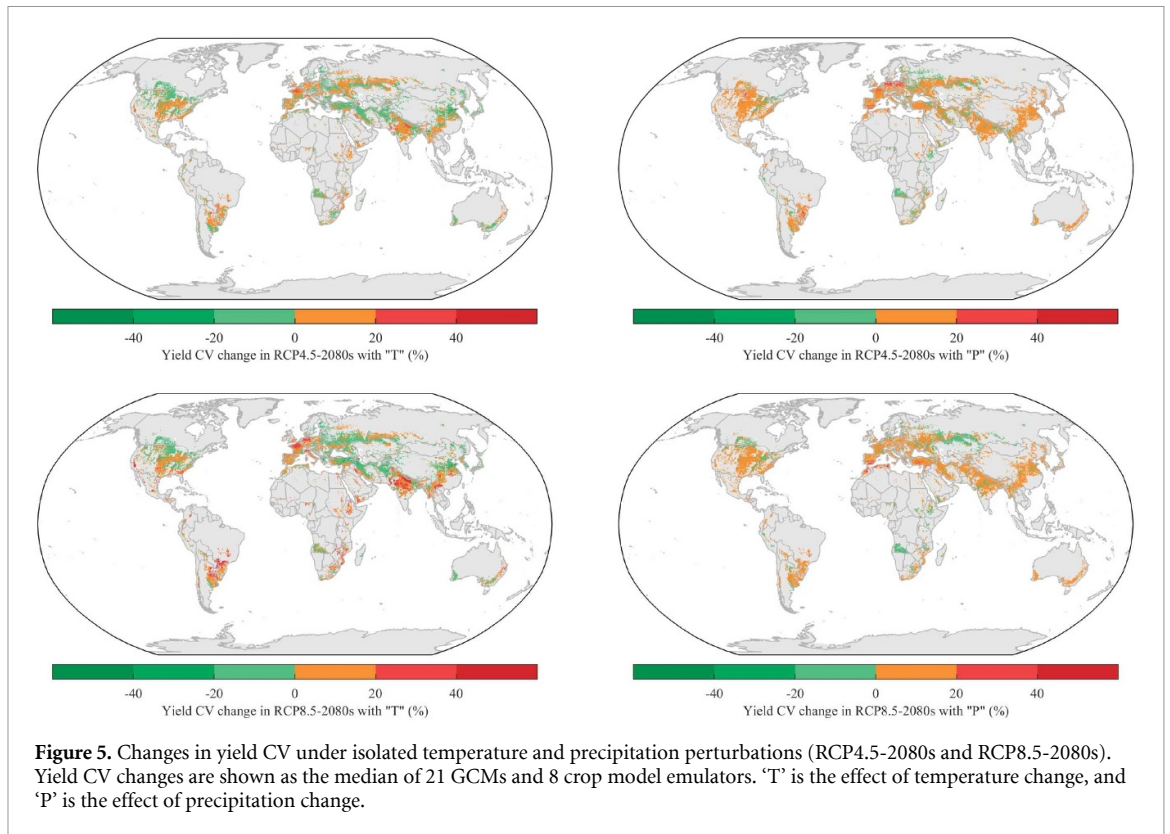

Figure 4. Wheat yield CV change under RCP4.5 and RCP8.5, separated by different climatic and management bins: growing season mean temperature (a), growing season total precipitation (b), and nitrogen fertilizer application (c). The bin classification refers to baseline reference conditions. CV change is based on the T + P + CO_2 simulations. Box-and-whisker plots show the distribution of yield CV changes across all cultivated grid cells in each class. The group divisions are based on approximately equal sample sizes.

wetter regions. Underperforming wheat production system regions, like Brazil, sub-Saharan Africa, and South East Asia, with lower levels of nitrogen application, are likely to experience a greater increase in yield CV under both RCP4.5 and RCP8.5.

3.3. Climatic drivers of and their relative contributions to the change in yield CV

In simulations based on individual climate drivers, temperature changes alone increase the yield CV for 55% and 56% of the harvested areas under RCP4.5-2080s and RCP8.5-2080s, respectively. Under RCP8.5-2080s the magnitude of increased yield CV with temperature change alone is larger than that with precipitation change alone, but the extent of the area affected by increasing yield CV is smaller (figure 5). The yield CV increases in 64% and 60% of harvested areas when only precipitation change is assumed under RCP4.5-2080s and RCP8.5-2080s, respectively (figure 5).

Figure 5. Changes in yield CV under isolated temperature and precipitation perturbations (RCP4.5-2080s and RCP8.5-2080s). Yield CV changes are shown as the median of 21 GCMs and 8 crop model emulators. 'T' is the effect of temperature change, and 'P' is the effect of precipitation change.

After separating the relative contributions of climate drivers (without elevated CO_2 concentration) under RCP4.5-2080s, precipitation was the dominant driver to increase the yield CV in 33% of harvested areas, even if the temperature change plays a more important role in yield CV change in over half of harvested areas (53%). The interaction between temperature and precipitation change played a dominant role in changes in yield CV in 10% of harvested areas. Under RCP8.5-2080s, temperature becomes a more important factor and was found to be the dominant driver in 72% of global wheat harvested areas, of which, yield CV increased in 41% of harvested areas. Precipitation was found to be the dominant driver in 21% of harvested areas, of which, yield CV increased in 17% of harvested areas. The interaction between temperature and precipitation played a dominant role in the change in yield CV in only 8% harvested areas (figure 6).

The elevated CO_2 concentration reduced the increase in yield CV, which was greatest in RCP8.5-2080s. The effect was strongest (>15%) in central Europe, south Asia, North and Southwest China, and North America. The mitigation effect was weaker under the other RCP4.5-2080s, but the spatial patterns were largely consistent with RCP8.5-2080s (figure 7).
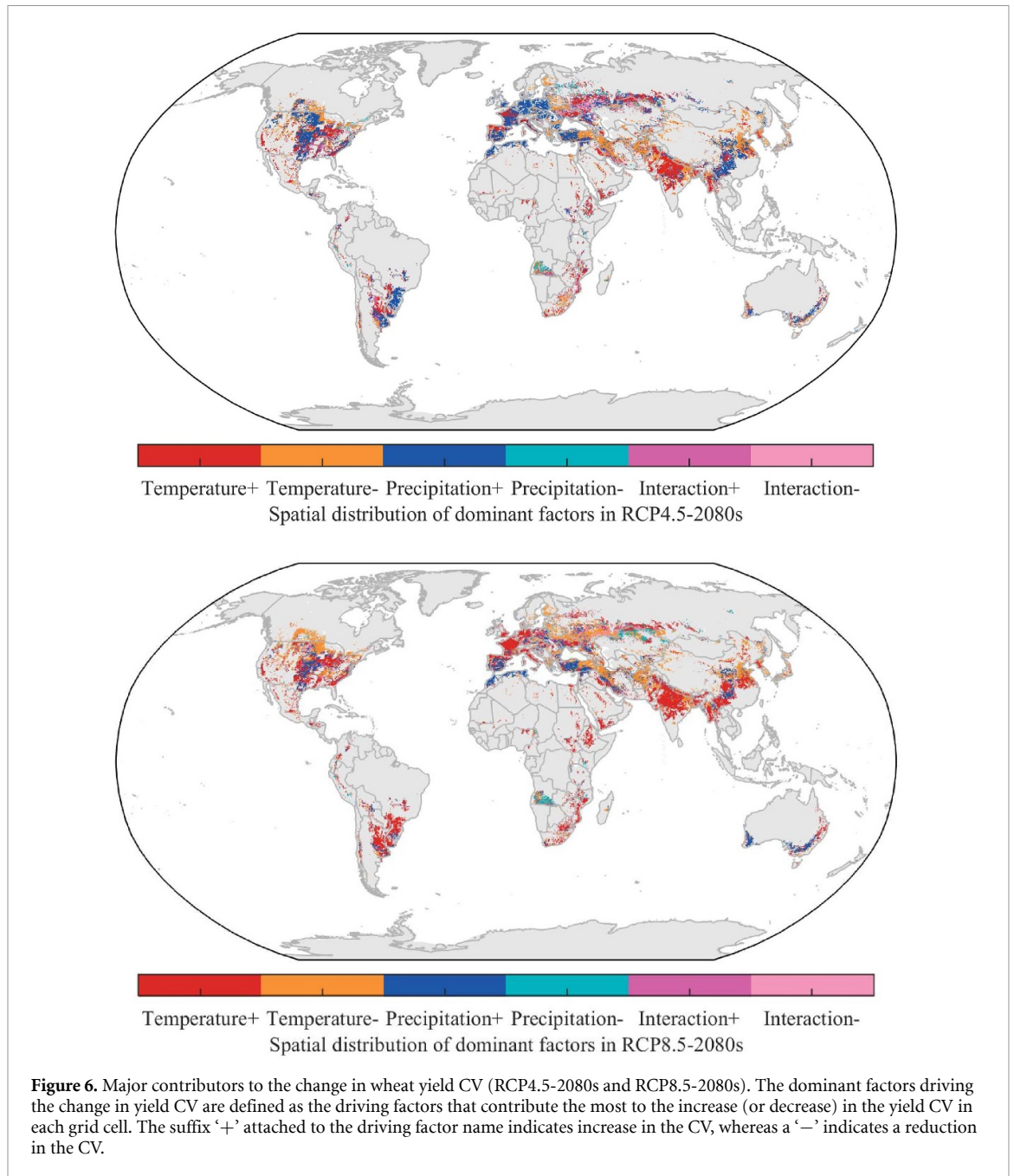
To elucidate the link between changes in yield CV and climate factors, we further examined the change in yield CV with climatic factors changes in mean, variability, and extremes of temperature and precipitation by using perturbation 'T' and 'P' results.

A linear regression was conducted between median changes in yield CV and growing season climatic factors from food producing units (FPUs, Kummu *et al* 2010) (figure 8). The change in yield CV was positively correlated with change in interannual variability (T_{gs}interV, figure 8(c)), intra-seasonal variability (T_{gs}intraV, figure 8(d)), and extreme degree day (EDD$_{gs}$, figure 8(e)) of temperature. The relationship between mean temperature and yield CV varied by region. For regions with hotter growing seasons (T_{gs}mean > 10 °C, figure 8(a)), a warming trend tended to increase the yield CV, and decrease the yield CV in regions with colder growing season (T_{gs}mean < 10 °C, figure 8(b)). For the effect of precipitation change, results from grid cells with rainfed systems showed that change in yield CV was negatively correlated with change in total precipitation (P_{gs}mean, figure 8(f)), but positively correlated with interannual variability of precipitation (P_{gs}interCV, figure 8(g)), and drought intensity (consecutive drought days, CDD$_{gs}$, figure 8(h)), all statistically significant.

4. Discussion

### 4.1. Changes in future wheat yield variability

Our results indicate that wheat yield CV might increase significantly in 18% of the global harvested area under a high-emission climate change scenario. In turn, yield variability is found to decrease in 44% of currently cultivated areas, regions in which mean yields are projected to increase under climate change.

Figure 6. Major contributors to the change in wheat yield CV (RCP4.5-2080s and RCP8.5-2080s). The dominant factors driving the change in yield CV are defined as the driving factors that contribute the most to the increase (or decrease) in the yield CV in each grid cell. The suffix '+' attached to the driving factor name indicates increase in the CV, whereas a '−' indicates a reduction in the CV.

Globally, our findings are consistent with those of earlier studies indicating that declining yield variability is wide-spread but increasing yield variability is found across important breadbasket regions (Iizumi and Ramankutty 2016, Leng 2017). Site-based simulation results for a 2 °C warming scenario (Liu *et al* 2019) have provided a more pessimistic estimation, with wheat yield CV increases in 36 out of the 60 sites, including the CO_2 fertilization effect. Our results confirm higher yield variability in hot regions as reported by (Liu *et al* 2019) and in regions with low nitrogen fertilizer application rates as reported by (Han *et al* 2020). Similarly, the low yield CV in high nitrogen fertilizer application rates regions is consistent with the findings of nutrients-driven intensification
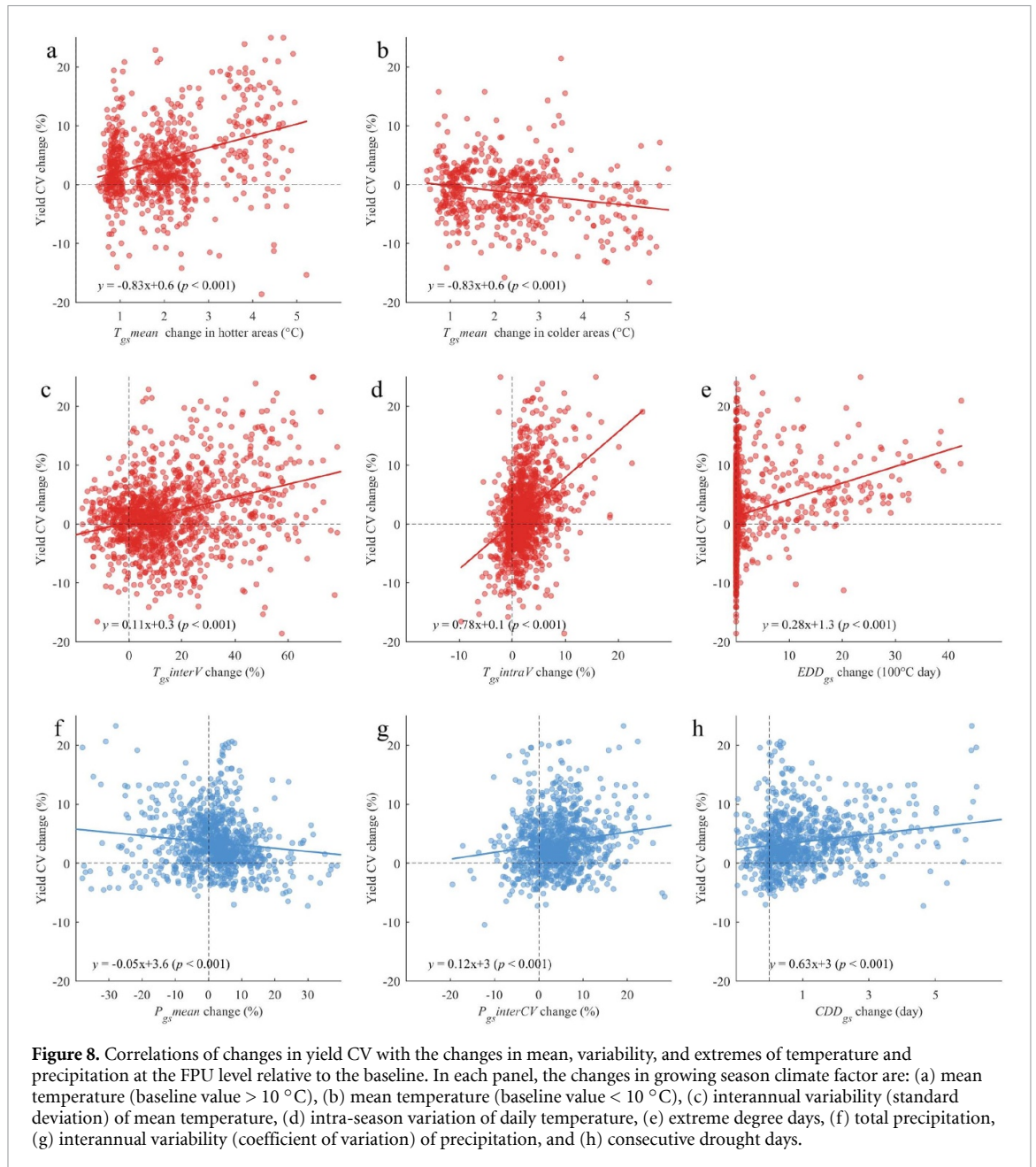
that additional nutrient inputs raise mean crop yields and thus decrease yield CV (Müller *et al* 2018).

A detailed comparison of yield CV changes between site-based projections (Liu *et al* 2019) and our gridded projections demonstrates the importance of revealing spatial heterogeneity of yield variability changes. Changes in yield CV were identified as significantly increasing at all 14 sites for the 2 °C warming scenario (Liu *et al* 2019). Among the 14 sites, our estimates were consistent with 10 of the 14 stations. For the other 46 sites, our results are largely consistent with the 25 sites across the central U.S., South America, the Middle East, the western European coastline, and Southern Russia; but are different in the direction

Figure 7. Reduction effect ('T + P + CO$_2$'−'T + P') on change in yield CV from CO$_2$ fertilization.
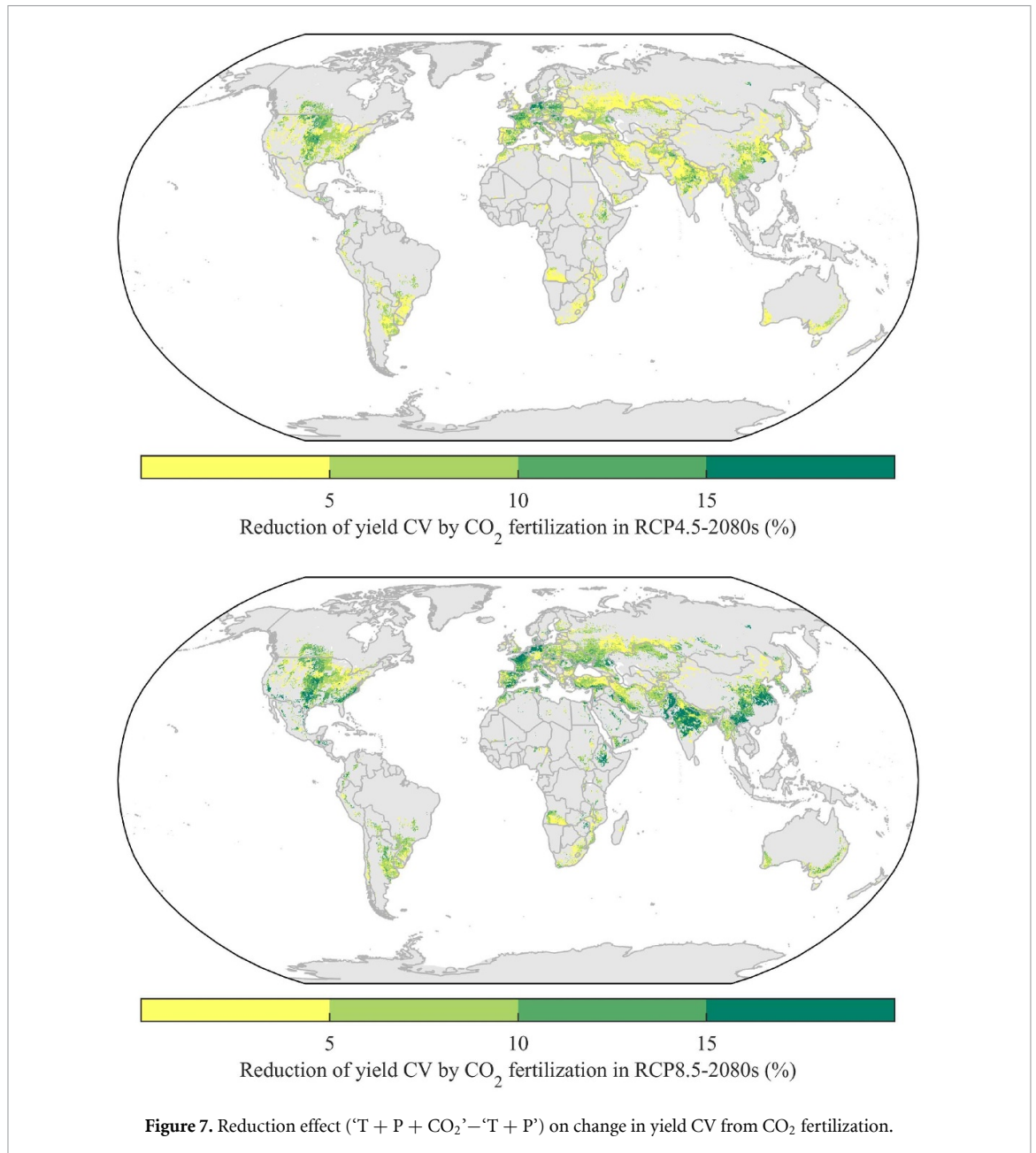
of change for other sites. Spatial heterogenous yield variability changes are the main cause of inconsistence between our projections and Liu *et al* (2019). This is the case in Glen and Bloemfontein in South Africa, and Dharwar in India for the four inconsistent sites, as well as 11 out of the other 21 inconsistent sites, including those in northwest US, around the western or northern coast of the Black Sea, in central southern Russia, North China, and south-eastern Australia. Besides, another cause may be the choice of the crop model ensemble and underlying uncertainties. We examined our results for each crop model emulator. The direction of each site-based change in yield CV reported by Liu *et al* (2019) can be found in the result of at least one of our emulators, indicating GCMs-crop models ensemble combination is critical to yield projection.

Spatial heterogeneity of crop yield variability creates a huge challenge for agricultural risk management (Benami *et al* 2021). The spatially heterogeneous yield CV changes are also found in earlier reports that yield variability changes in rice and wheat are sensitive to spatial resolution (Iizumi *et al* 2018). Previous yield variability projections conducted with site-based, process-based models have found that regional yield variability changes are not consistent across different sites (Liu *et al* 2021). Thus, the gridded process-based crop models can provide an overview of global or regional changes in yield variability (Ostberg *et al* 2018, Parkes *et al* 2018). The ability to represent this spatial heterogeneity in yield variability in light-weight emulators allows for more comprehensive assessments of the risk of changes in yield variability.

Figure 8. Correlations of changes in yield CV with the changes in mean, variability, and extremes of temperature and precipitation at the FPU level relative to the baseline. In each panel, the changes in growing season climate factor are: (a) mean temperature (baseline value > 10 °C), (b) mean temperature (baseline value < 10 °C), (c) interannual variability (standard deviation) of mean temperature, (d) intra-season variation of daily temperature, (e) extreme degree days, (f) total precipitation, (g) interannual variability (coefficient of variation) of precipitation, and (h) consecutive drought days.

4.2. Climatic drivers of changes in future wheat yield variability

The present results indicate strong links between changes in the wheat yield CV and changes in temperature and precipitation. Previous reports have suggested that changes in yield interannual variability are closely related to changes in the variability (both interannual and intra-seasonal) (Iizumi *et al* 2013, Peng *et al* 2018) and extremes of climate factors (Iizumi and Ramankutty 2016, Chen *et al* 2018). In addition, due to the non-linear relationship between yield and temperature, changes in the mean temperature, away from the optimal range, will increase the interannual yield CV (Urban *et al* 2012, Tigchelaar *et al* 2018). The response of the interannual yield variability to changes in precipitation is more complex

than for temperature. In general, changes in precipitation have smaller effects on irrigated yield than on rainfed yield (Tubiello *et al* 2002, Kothari *et al* 2019). In rainfed systems, yield interannual variability has been known to be closely related to interannual variability of rainfall, as well as frequency and intensity of drought (Webber *et al* 2018). The effect of total precipitation change largely depends on the baseline humidity of the production region. For drylands, increasing total precipitation increases mean yield (Fronzek *et al* 2018) and consequently reduces CV. Also, the interaction between temperature and precipitation changes can mitigate the increase in yield CV, although the magnitude of the interaction effect on change in yield CV is modest, within 10%. This is similar to the mitigation effect of irrigation

on heat stress (Zaveri and Lobell 2019). However, the interaction effect cannot be explicitly explained, depending on the timing, intensity, and volume of rainfall (Tack *et al* 2017).

Higher atmospheric CO_2 concentrations mitigate variability changes in crop yield (Urban *et al* 2015), a consistent finding across different scenarios and time periods (figure 7). The mitigation effect is mainly attributed to increases in mean crop yield under elevated CO_2. Wheat as a C3 crop is known to have a high capacity to benefit from elevated CO_2 levels, which has been confirmed by various previous experiment-based evidences (Kimball 2016, Toreti *et al* 2020). Negative effects of global warming on future wheat yield could potentially be fully compensated by yield-amplifying effects of elevated atmospheric CO_2 concentrations (Ye *et al* 2020).

4.3. Uncertainties

The spatial pattern of uncertainty in our results is consistent with different uncertainty distribution between high and low latitudes provided by crop model simulation (Xiong *et al* 2020). Including the CO_2 fertilization effect would further increase the total size of uncertainty in the projected yield. This is in agreement with a recent analysis on sources of uncertainty regarding GCMs and GGCM statistical emulators (Müller *et al* 2021).

The use of emulator ensemble simulation enabled the estimation of wheat yield variability change driven by climate change. Nevertheless, our approach has two limitations. First, crop damage from climate extremes is a major driving force of interannual yield variability (Trnka *et al* 2014), but the capability of most crop models in reproducing extreme climate damage to crops is still limited (Rötter *et al* 2018). For instance, process-based crop models of the GGCMI phase 1 experiment fail to reproduce yield impact from too wet conditions (Li *et al* 2019). Also, process-based crop models underestimate the extremeness of the 2003 heat-drought (Schewe *et al* 2019). We employ newly developed crop model emulators to project future wheat yield and these emulators are capable of capturing the direction of yield anomalies due to climate extremes, indicating the type of extreme event-induced yield variability that is captured by the models (heat, drought) will increase yield variability in a fair share of current cropland. Second, interannual yield variability driven by non-climatic factors is not considered in our analysis. These non-climatic factors can strongly affect yield variability (Albers *et al* 2017) and changes in management can also strongly affect yield levels under climate change (Minoli *et al* 2019, Zabel *et al* 2021).

4.4. Implications

The spatial scale of our estimates reached the sub-province scale in China and the sub-state scale in the

US and thus provided more insight than previous global estimates. First, gridded estimated yield variability change could provide more detail on spatial heterogeneity in local areas. Such local spatial differences were pronounced in South Africa, eastern Africa, and Central Russia. Second, when there is a need to estimate regional or country-level aggregated yield variability change, our gridded estimates could enable straightforward aggregation rather than upscaling from site-based estimates—these estimates rely heavily on the representativeness of sites.

High-spatial resolution gridded estimates of future yield variability change enabled global estimates of future change in yield CV. Globally, changes in yield CV tend to decrease in 44% of global harvested areas; but still yields would become more unstable in 18% of global harvested areas under RCP8.5-2080s, including several major production regions and countries. This indicates potential challenges to the stability of grain supply, market price, and consequently, the whole food system in the context of future climate change. It is important for local and regional economies to proactively implement adaptation measures and policy support (Iizumi and Ramankutty 2016). In light of this, our results can provide details of spatial heterogeneity in local areas and identify regions with urgent needs, including those hot and low-fertilizer application regions. The predominant climate driver is also identified, so that adaptation strategies can be tailored for regional or local challenges.

To face the challenge of increased yield inter-annual variability, adaptations including mean-increasing and variance-reducing strategies (Mehrabi and Ramankutty 2019), are needed because the changes in relative yield variability (CV) are sourced from both changes in mean yield and yield standard deviation (figure S9). The focus on the relative yield variability (CV) rather than absolute (e.g. SD) reflects the producer perspective, where the variability around the mean is relevant (storage and financial buffers) even if the mean is increasing in the long-term (Hasegawa *et al* 2021). Shifting cultivars (Liu *et al* 2010, Olmstead and Rhode 2011), changing sowing regions (Iizumi *et al* 2021) and adjusting planting dates (Lobell 2014, Huang *et al* 2020) have been recognized as effective adaptation options to address heat stress. Likewise, reinforcing irrigation equipment and adjusting irrigation strategies could relieve water shortages (Zhao *et al* 2020). Additionally, increasing nitrogen application rates in under-performing wheat production system regions could mitigate the increase in yield CV (Han *et al* 2020). From a risk management perspective, the risk in increased yield CV requires better domestic inter-temporal reserves of wheat grain to smooth fluctuations in interannual production, market supply, and commodity price and better financial buffers at the

producer level, to mitigate financial losses from local less-than-average yields.

5. Conclusions

This study presents one of the first projections of future wheat yield interannual variability change at high spatial resolution and disentangles the impacts from changes in temperature, precipitation, and CO_2 on those changes. Our results reveal that future climate change alters wheat yield interannual variability in over 60% of harvested areas. Wheat yield variability may decrease in over 40% of global wheat harvested areas under a high-emission climate change scenario (RCP8.5-2080s), while under RCP4.5-2080s only 31% of harvested areas undergo the declined yield CV. However, 23% and 18% of harvested areas experience increased yield CV under RCP4.5-2080s and RCP8.5-2080s, respectively. Greater increase in yield standard deviation than that in the mean yield was the main reason for the increase yield variability under both RCP4.5 and RCP8.5. Yields in hotter or lower fertilizer regions are projected to become more unstable. Worldwide, changes in temperature have a stronger influence on changes in yield variability compared with precipitation in 72% of global harvested areas under RCP8.5-2080s, whereas under RCP4.5-2080s the areas controlled by temperature changes are smaller (predominant in 53% of harvested areas). The global mean of yield CV reduction due to rising CO_2 concentration across current harvested areas are 5% and 8% under RCP4.5-2080s and RCP8.5-2080s, respectively. High spatial resolution patterns of changes in wheat yield variability, as well as site-specific major driver identification results, have great implications for policy-making with regard to where food supply and farmer income need to be stabilized by additional measures in wheat production throughout the world.

Data availability statement

The data that support the findings of this study are available upon reasonable request from the authors.

Acknowledgment

ORCID iDs

Tao Ye ⓘ https://orcid.org/0000-0002-5037-8410
Jonas Jägermeyr ⓘ https://orcid.org/0000-0002-8368-0018
Christoph Müller ⓘ https://orcid.org/0000-0002-9491-3550

References

Albers H, Gornott C and Hüttel S 2017 How do inputs and weather drive wheat yield volatility? The example of Germany *Food Policy* **70** 50–61

Ben-Ari T, Boé J, Ciais P, Lecerf R, Van Der Velde M and Makowski D 2018 Causes and implications of the unforeseen 2016 extreme yield loss in the breadbasket of France *Nat. Commun.* **9** 1627

Benami E, Jin Z, Carter M R, Ghosh A, Hijmans R J, Hobbs A, Kenduiywo B and Lobell D B 2021 Uniting remote sensing, crop modelling and economics for agricultural risk management *Nat. Rev. Earth Environ.* **2** 140–59

Blanc É 2017 Statistical emulators of maize, rice, soybean and wheat yields from global gridded crop models *Agric. For. Meteorol.* **236** 145–61

Blanc E and Sultan B 2015 Emulating maize yields from global gridded crop models using statistical estimates *Agric. For. Meteorol.* **214–215** 134–47

Campbell B M *et al* 2016 Reducing risks to food security from climate change *Glob. Food Sec.* **11** 34–43

Ceglar A, Toreti A, Lecerf R, Van Der Velde M and Dentener F 2016 Impact of meteorological drivers on regional inter-annual crop yield variability in France *Agric. For. Meteorol.* **216** 58–67

Challinor A J, Watson J, Lobell D B, Howden S M, Smith D R and Chhetri N 2014 A meta-analysis of crop yield under climate change and adaptation *Nat. Clim. Change* **4** 287–91

Chen Y, Zhang Z and Tao F 2018 Impacts of climate change and climate extremes on major crops productivity in China at a global warming of 1.5 and 2.0 °C *Earth Syst. Dyn.* **9** 543–62

Döring T F and Reckling M 2018 Detecting global trends of cereal yield stability by adjusting the coefficient of variation *Eur. J. Agron.* **99** 30–36

Elliott J *et al* 2015 The global gridded crop model intercomparison: data and modeling protocols for phase 1 (v1.0) *Geosci. Model Dev.* **8** 261–77

FAO 2019 World food and agriculture statistical pocketbook

Folberth C, Baklanov A, Balkovič J, Skalský R, Khabarov N and Obersteiner M 2019 Spatio-temporal downscaling of gridded crop model yield estimates based on machine learning *Agric. For. Meteorol.* **264** 1–15

Franke J A *et al* 2020a The GGCMI Phase 2 emulators: global gridded crop model responses to changes in CO_2, temperature, water, and nitrogen (version 1.0) *Geosci. Model Dev.* **13** 3995–4018

Franke J A *et al* 2020b The GGCMI phase 2 experiment: global gridded crop model simulations under uniform changes in CO2, temperature, water, and nitrogen levels (protocol version 1.0) *Geosci. Model Dev.* **13** 2315–36

Fronzek S *et al* 2018 Classifying multi-model wheat yield impact response surfaces showing sensitivity to temperature and precipitation change *Agric. Syst.* **159** 209–24

Han X, Hu C, Chen Y, Qiao Y, Liu D, Fan J, Li S and Zhang Z 2020 Crop yield stability and sustainability in a rice-wheat cropping system based on 34-year field experiment *Eur. J. Agron.* **113** 125965

Hasegawa T, Sakurai G, Fujimori S, Takahashi K, Hijioka Y, Masui T 2021 Extreme climate events increase risk of global food insecurity and adaptation needs *Nat. Food* **2** 587–595

Hawkins E, Fricker T E, Challinor A J, Ferro C A T, Ho C K and Osborne T M 2013 Increasing influence of heat stress on French maize yields from the 1960s to the 2030s *Glob. Change Biol.* **19** 937–47

Holzkämper A, Calanca P and Fuhrer J 2012 Statistical crop models: predicting the effects of temperature and precipitation changes *Clim. Res.* **51** 11–21

Huang M, Wang J, Wang B, Liu D L, Yu Q, He D, Wang N and Pan X 2020 Optimizing sowing window and cultivar choice can boost China's maize yield under 1.5 °C and 2 °C global warming *Environ. Res. Lett.* **15** 024015

Iizumi T, Ali-Babiker I A, Tsubo M, Tahir I S, Kurosaki Y, Kim W, Gorafi Y S, Idris A A and Tsujimoto H 2021 Rising temperatures and increasing demand challenge wheat supply in Sudan *Nat. Food* **2** 19–27

Iizumi T, Kotoku M, Kim W, West P C, Gerber J S and Brown M E 2018 Uncertainties of potentials and recent changes in global yields of major crops resulting from census- and satellite-based yield datasets at multiple resolutions *PLoS One* **13** e0203809

Iizumi T and Ramankutty N 2016 Changes in yield variability of major crops for 1981–2010 explained by climate change *Environ. Res. Lett.* **11** 34003

Iizumi T, Sakuma H, Yokozawa M, Luo J J, Challinor A J, Brown M E, Sakurai G and Yamagata T 2013 Prediction of seasonal climate-induced variations in global food production *Nat. Clim. Change* **3** 904–8

IPCC 2014 Climate change 2014: synthesis report

IPCC 2019 Climate change and land: an IPCC special report on climate change, desertification, land degradation, sustainable land management, food security, and greenhouse gas fluxes in terrestrial ecosystems

Jägermeyr J *et al* 2021 Climate change signal in global agriculture emerges earlier in new generation of climate and crop models *Nat. Food* (https://doi.org/10.21203/rs.3.rs-101657/v1) (*Accepted*)

Kimball B A 2016 Crop responses to elevated CO_2 and interactions with H_2O, N, and temperature *Curr. Opin. Plant Biol.* **31** 36–43

Knapp S and Van Der Heijden M G A 2018 A global meta-analysis of yield stability in organic and conservation agriculture *Nat. Commun.* **9** 1–9

Kothari K, Ale S, Attia A, Rajan N, Xue Q and Munster C L 2019 Potential climate change adaptation strategies for winter wheat production in the Texas High Plains *Agric. Water Manage.* **225** 105764

Kucharik C J and Ramankutty N 2005 Trends and variability in U.S. Corn yields over the twentieth century *Earth Interact.* **9** 1–29

Kummu M, Ward P J, De Moel H and Varis O 2010 Is physical water scarcity a new phenomenon? Global assessment of water shortage over the last two millennia *Environ. Res. Lett.* **5** 34006

Leng G 2017 Recent changes in county-level corn yield variability in the United States from observations and crop models *Sci. Total Environ.* **607–608** 683–90

Leng G and Hall J W 2020 Predicting spatial and temporal variability in crop yields: an inter-comparison of machine learning, regression and process-based models *Environ. Res. Lett.* **15** 44027

Li Y, Guan K, Schnitkey G D, DeLucia E and Peng B 2019 Excessive rainfall leads to maize yield loss of a comparable magnitude to extreme drought in the United States *Glob. Change Biol.* **25** 2325–37

Liu B *et al* 2019 Global wheat production with 1.5 and 2.0 °C above pre-industrial warming *Glob. Change Biol.* **25** 1428–44

Liu W, Ye T and Shi P 2021 Decreasing wheat yield stability on the North China Plain: relative contributions from climate change in mean and variability *Int. J. Climatol.* **41** (Suppl. 1): E2820–E33

Liu Y, Wang E, Yang X and Wang J 2010 Contributions of climatic and crop varietal changes to crop production in the North China Plain, since 1980s *Glob. Change Biol.* **16** 2287–99

Lobell D B 2014 Climate change adaptation in crop production: beware of illusions *Glob. Food Sec.* **3** 72–76

Lobell D B and Burke M B 2010 On the use of statistical models to predict crop yield responses to climate change *Agric. For. Meteorol.* **150** 1443–52

Lobell D B, Roberts M J, Schlenker W, Braun N, Little B B, Rejesus R M and Hammer G L 2014 Greater sensitivity to drought accompanies maize yield increase in the U.S. Midwest *Science* **344** 516–9

Lobell D B, Schlenker W and Costa-Roberts J 2011 Climate trends and global crop production since 1980 *Science* **333** 616–20

Martre P *et al* 2015 Multimodel ensembles of wheat growth: many models are better than one *Glob. Change Biol.* **21** 911–25

Matiu M, Ankerst D P and Menzel A 2017 Interactions between temperature and drought in global and regional crop yield variability during 1961–2014 *PLoS One* **12** e0178339

Mehrabi Z and Ramankutty N 2019 Synchronized failure of global crop production *Nat. Ecol. Evol.* **3** 780–6

Minoli S *et al* 2019 Global response patterns of major rainfed crops to adaptation by maintaining current growing periods and irrigation *Earth's Future* **7** 1464–80

Moriondo M, Giannakopoulos C and Bindi M 2011 Climate change impact assessment: the role of climate extremes in crop yield simulation *Clim. Change* **104** 679–701

Müller C *et al* 2017 Global gridded crop model evaluation: benchmarking, skills, deficiencies and implications *Geosci. Model Dev.* **10** 1403–22

Müller C *et al* 2018 Global patterns of crop yield stability under additional nutrient and water inputs *PLoS One* **13** e0198748

Müller C *et al* 2021 Exploring uncertainties in global crop yield projections in a large ensemble of crop models and CMIP5 and CMIP6 climate scenarios *Environ. Res. Lett.* **16** 034040

Olmstead A L and Rhode P W 2011 Adapting North American wheat production to climatic challenges, 1839–2009 *Proc. Natl Acad. Sci.* **108** 480–5

Osborne T M and Wheeler T R 2013 Evidence for a climate signal in trends of global crop yield variability over the past 50 years *Environ. Res. Lett.* **8** 024001

Ostberg S, Schewe J, Childers K and Frieler K 2018 Changes in crop yields and their variability at different levels of global warming *Earth Syst. Dyn.* **9** 479–96

Oyebamiji O K, Edwards N R, Holden P B, Garthwaite P H, Schaphoff S and Gerten D 2015 Emulating global climate change impacts on crop yields *Stat. Model.* **15** 499–525

Parkes B, Defrance D, Sultan B, Ciais P and Wang X 2018 Projected changes in crop yield mean and variability over West Africa in a world 1.5 K warmer than the pre-industrial era *Earth Syst. Dyn.* **9** 119–34

Peng B, Guan K, Pan M and Li Y 2018 Benefits of seasonal climate prediction and satellite data for forecasting U.S. maize yield *Geophys. Res. Lett.* **45** 9662–71

Portmann F T, Siebert S and Döll P 2010 MIRCA2000—global monthly irrigated and rainfed crop areas around the year 2000: a new high-resolution data set for agricultural and hydrological modeling *Glob. Biogeochem. Cycles* **24** GB1011

Raimondo M, Nazzaro C, Marotta G and Caracciolo F 2021 Land degradation and climate change: global impact on wheat yields *Land Degrad. Dev.* **32** 387–98

Ray D K, Gerber J S, Macdonald G K and West P C 2015 Climate variation explains a third of global crop yield variability *Nat. Commun.* **6** 5989

Ringeval B, Müller C, Pugh T, Mueller N, Ciais P, Folberth C, Liu W, Debaeke P and Pellerin S 2021 Potential yield simulated by global gridded crop models: a process-based emulator to explain their differences *Geosci. Model Dev. Discuss.* **14** 1639–56

Rosenzweig C *et al* 2014 Assessing agricultural risks of climate change in the 21st century in a global gridded crop model intercomparison *Proc. Natl Acad. Sci.* **111** 3268–73

Rötter R P, Appiah M, Fichtler E, Kersebaum K C, Trnka M and Hoffmann M P 2018 Linking modelling and experimentation to better capture crop impacts of agroclimatic extremes—a review *F. Crop. Res.* **221** 142–56

Ruane A C, Goldberg R and Chryssanthacopoulos J 2015 Climate forcing datasets for agricultural modeling: merged products for gap-filling and historical climate series estimation *Agric. For. Meteorol.* **200** 233–48

Sacks W J, Deryng D, Foley J A and Ramankutty N 2010 Crop planting dates: an analysis of global patterns *Glob. Ecol. Biogeogr.* **19** 607–20

Schewe J *et al* 2019 State-of-the-art global models underestimate impacts from climate extremes *Nat. Commun.* **10** 1–14

Schlenker W and Roberts M J 2009 Nonlinear temperature effects indicate severe damages to U.S. crop yields under climate change *Proc. Natl Acad. Sci. USA* **106** 15594–8

Sternberg T 2011 Regional drought has a global impact *Nature* **472** 169

Tack J, Barkley A and Hendricks N 2017 Irrigation offsets wheat yield reductions from warming temperatures *Environ. Res. Lett.* **12** 114027

Tao F, Zhang Z, Zhang S and Rötter R P 2016 Variability in crop yields associated with climate anomalies in China over the past three decades *Reg. Environ. Change* **16** 1715–23

Taylor K E, Stouffer R J and Meehl G A 2012 An Overview of CMIP5 and the Experiment Design *Bulletin of the American Meteorological Society* **93** 485–98

Thrasher B L 2012 Technical note: bias correcting climate model simulated daily temperature extremes with quantile mapping *Hydrol. Earth Syst. Sci. Discuss.* **9** 5515–29

Tigchelaar M, Battisti D S, Naylor R L and Ray D K 2018 Future warming increases probability of globally synchronized maize production shocks *Proc. Natl Acad. Sci.* **115** 6644–9

Toreti A *et al* 2020 Narrowing uncertainties in the effects of elevated CO_2 on crops *Nat. Food* **1** 775–82

Trnka M, Rötter R P, Ruiz-Ramos M, Kersebaum K C, Olesen J E, Žalud Z and Semenov M A 2014 Adverse weather conditions for European wheat production will become more frequent with climate change *Nat. Clim. Change* **4** 637–43

Tubiello F N, Rosenzweig C, Goldberg R A, Jagtap S and Jones J W 2002 Effects of climate change on US crop production: simulation results using two different GCM scenarios. Part I: wheat, potato, maize, and citrus *Clim. Res.* **20** 259–70

Urban D W, Sheffield J and Lobell D B 2015 The impacts of future climate and carbon dioxide changes on the average and variability of US maize yields under two emission scenarios *Environ. Res. Lett.* **10** 045003

Urban D, Roberts M J, Schlenker W and Lobell D B 2012 Projected temperature changes indicate significant increase in interannual variability of U.S. maize yields: a letter *Clim. Change* **112** 525–33

Webber H *et al* 2018 Diverging importance of drought stress for maize and winter wheat in Europe *Nat. Commun.* **9** 4249

Wheeler T and Von Braun J 2013 Climate change impacts on global food security *Science* **341** 508–13

Xiong W, Asseng S, Hoogenboom G, Hernandez-Ochoa I, Robertson R, Sonder K, Pequeno D, Reynolds M and Gerard B 2020 Different uncertainty distribution between high and low latitudes in modelling warming impacts on wheat *Nat. Food* **1** 63–69

Ye Z *et al* 2020 Impacts of 1.5 °C and 2.0 °C global warming above pre-industrial on potential winter wheat production of China *Eur. J. Agron.* **120** 126149

You L, Wood S, Wood-Sichra U and Wu W 2014 Generating global crop distribution maps: from census to grid *Agric. Syst.* **127** 53–60

Yue Y, Zhang P and Shang Y 2019 The potential global distribution and dynamics of wheat under multiple climate change scenarios *Sci. Total Environ.* **688** 1308–18

Zabel F *et al* 2021 Large potential for crop production adaptation depends on available future varieties *Glob. Change Biol* **27** 3870–82

Zaveri E and Lobell D B 2019 The role of irrigation in changing wheat yields and heat sensitivity in India *Nat. Commun.* **10**

Zhao J, Han T, Wang C, Jia H, Worqlul A W, Norelli N, Zeng Z and Chu Q 2020 Optimizing irrigation strategies to synchronously improve the yield and water productivity of winter wheat under interannual precipitation variability in the North China Plain *Agric. Water Manage.* **240** 106298

Zhu P, Zhuang Q, Archontoulis S V, Bernacchi C and Müller C 2019 Dissecting the nonlinear response of maize yield to high temperature stress with model-data integration *Glob. Change Biol.* **25** 2470–84